

Particle size effects in the antiferromagnetic spinel CoRh_2O_4

R. N. Bhowmik^{a*}, R. Nagarajan^b and R. Ranganathan^a

^a*Experimental Condensed Matter Physics Division,*

Saha Institute of Nuclear Physics, 1/AF, Bidhannagar, Calcutta 700064, India

and

^b*Tata Institute of Fundamental Research, Solid State Condensed Matter Physics*

Division, Mumbai, India

Abstract

We report the particle size dependent magnetic behaviour in the antiferromagnetic spinel CoRh_2O_4 . The nanoparticles were obtained by mechanical milling of bulk material, prepared under sintering method. The XRD spectra show that the samples are retaining the spinel structure. The particle size decreases from 70 nm to 16 nm as the milling time increases from 12 hours upto 60 hours. The magnetic measurements suggest that the antiferromagnetic ordering at $T_N \approx 27\text{K}$ exists in bulk as well as in nanoparticle samples. However, the magnitude of the magnetization below T_N increases with decreasing particle size. Considering the fact that Rh^{3+} has strong octahedral (B) site occupation and no change in T_N of bulk and nanoparticle samples, we believe that the observed magnetic enhancement is not related to the cationic redistribution between tetrahedral (A) and octahedral (B) sites of the spinel structure. In our opinion, the observed effect is a consequence of decreasing coherent length of antiferromagnetic coupled core spins and increasing number of the frustrated shell in the core-shell model of anoparticle.

*e-mail:rnb@cmp.saha.ernet.in

I. INTRODUCTION

The nanoparticle spinel ferrites are under the intensive investigation in recent years because of their potential applications in nanoscience and technology as high density magnetic recording media, magnetic carriers in ferro fluids, magnetically guided drug carrier etc. [1]. The theoretical interest for such type of materials are growing up to understand the structural and magnetic modifications taking place in a system when the dimension of the particles (crystal size) are reduced to atomic scale [2–5]. Several novel phenomena like magnetic quantum tunneling [2], superparamagnetism, surface spin canting [6], grain boundary effect [7], non-equilibrium cation distributions among the inequivalent lattice sites [8] are attracting the spinel ferrites. In spinel lattices the anions (O^{2-} , S^{2-} ions) form a cubic close packing, in which the interstices are occupied by tetrahedral (form A sites or sublattice) and octahedral (form B sites or sublattice) coordinated cations to the oxygen anions. The competition between various type of superexchange interactions via O^{2-} ions, *i.e.*, inter-sublattice superexchange interactions (J_{AB}) between ions of both sites and intra-sublattice superexchange interactions (J_{AA} and J_{BB}) between ions of same site, shows a variety of magnetic states like ferrimagnet/ferromagnet, antiferromagnet, superparamagnet and spin glass in spinel oxides [3]. When the particles size are reduced in the nanometer scale a drastically different kind of magnetic behaviour were observed in spinel oxides in comparison with the bulk material [5,9]. This has been explained in terms of site disorder, *i.e.*, the cations redistribution between A and B sites [10,11] and finite size scaling effect [12].

It is established that for long range ferrimagnetic ordering in spinel oxide, the necessary condition is $|J_{AB}| \gg |J_{BB}| \gg |J_{AA}|$ [13]. However, if we compare the antiferromagnetic ordering temperature (T_N) of two typical normal spinel antiferromagnets $ZnFe_2O_4$ with $T_N \sim 10K$ (where only J_{BB} exist) and $CoRh_2O_4$ with $T_N \approx 27K$ (where only J_{AA} exist) [14], it can be understood that $|J_{BB}| \gg |J_{AA}|$ may be true only for long range order ferrimagnetic spinels (where both A and B sites are occupied by magnetic ions) but not for all the cases, particularly, for the spinels with magnetic ion only on A site. Unfortunately, most of the

reports deal with the nanoparticle spinels where either B or both A and B sites are occupied by magnetic ions [8,6,10].

It will be very interesting to investigate the particle size effect on antiferromagnetic spinels with magnetic moment only on A sites. Recently, M. Sato et al. [15] reported the disappearance of antiferromagnetic ordering at 33K of bulk Co_3O_4 spinel and the appearance of a variety of magnetic phases like ferrimagnet, superparamagnet and spin glass when the particle size is reduced to nano scale. For Co_3O_4 spinel oxide, the B site is fully occupied by non-magnetic Co^{3+} ($3d^6$) ions and A site is occupied by magnetic Co^{2+} ions, which gives rise to long range antiferromagnetic order due to $\text{Co}^{2+}\text{-O}^{2-}\text{-Co}^{2+}$ (J_{AA}) superexchange interactions with $J_{AB} = J_{AA} = 0$ [15]. CoRh_2O_4 (structure: $(\text{Co}^{2+})_A[\text{Rh}^{3+}]_2\text{O}_4$) with $T_N \approx 27\text{K}$ is an anlogus of Co_3O_4 (structure: $(\text{Co}^{2+})_A[\text{Co}^{3+}]_2\text{O}_4$), where Co^{3+} is replaced by non-magnetic Rh^{3+} ($4d^6$) ions [14].

Recently, a significant research interest is focussing on the geometrically frustrated antiferromagnets (Ising or Heisenberg in nature). The change of degeneracy and topology of the antiferromagnetic ground state (Neel order) of such a system can show various kind of interesting magnetic properties such as quantum disordered ground states [16], quantum zero -temperature spin fluctuation effect, where the system do not order and remain in a "collective paramagnetic state" down to zero temperature [17]. The degeneracy of the antiferromagnetic ground states can be reduced by introducing random non-magnetic dilution [18] or by strain induced positional disorder [19]. Even some authors introduced the concept of ordering in geometrically frustrated system due to disorder while the degeneracy is reduced in the system [16,18]. Mechanical milling is one of the most convenient method which can introduce the positional disorder in the lattices and simultaneously reduce the particle size of the material.

In this paper, we address the nature of magnetic order as a function of particle size in CoRh_2O_4 prepared by mechanical milling. The samples are characterized by XRD and magnetization measurements have been performed using SQUID magnetometer.

II. EXPERIMENTAL

We have synthesized nano particles CoRh_2O_4 spinel oxide by mechanical milling of the bulk material using Fritsch Planetary Mono Mill "Pulverisette 6". For bulk material, the stoichiometric mixture of Co_3O_4 (99.5% from Fluka) and Rh_2O_3 (99.9 % from Johnson Matthey) oxides was taken for CoRh_2O_4 composition. The mixture was mechanically ground for 2 hours and was pelletized. The pelet was sintered at 1000°C for 12 hours and at 1200°C for 48 hours. The sample was then cooled to room temperature at $2\text{-}3^\circ\text{C}/\text{minute}$. A typical crystalline spinel structure was confirmed by X ray diffraction (XRD) spectra using Philips PW1710 diffractometer with Cu K_α radiation. The bulk material was powdered using a 80 ml agate vial with 10 mm agate balls. We intentionally did not use the stainless bowl and balls to avoid any kind of contamination of transition metals (Fe, Cr, Ni). The samples were milled with ball to powder mass ratio 12:1 and at a rotational speed of 300 rpm. Small amount of samples were taken out from the bowl after 12 (mh12 sample), 24 (mh24 sample), 36 (mh36 sample), 48 (mh48 sample) and 60 (mh60 sample) hours of milling for our studies. The dc magnetization measurements were performed using SQUID (quantum design) magnetometer.

III. RESULTS AND DISCUSSION

A. Structural properties

The X ray diffraction spectra (Fig.1) show that the crystalline nature of bulk CoRh_2O_4 decreases with increasing milling time. It should be noted that the crystalline peaks of milled samples, as shown for 311 line (Fig. 1b), shows small shift to higher scattering angle (2θ) with respect to the bulk sample. However, there is no extra lines in XRD spectra for as milled samples in comparison with bulk sample. This suggests that small amount of lattice disorder or lattice strain is introduced in the system as the particle size is reduced by mechanical milling but without changing the crystal symmetry of spinel structure [20,21].

The decrease of lattice parameter (see Table 1) suggest that it is related with the decrease of particle size as a function of milling time [22]. The transmission electron micrographs (TEM) confirm the decrease of particle size from 70 nm (12 hours milling) to 16 nm (60 hours milling) (see Table 1). The broad lines in XRD spectra is due to this decrease of particle size, where the thermal fluctuation of the small coherent (crystalline) zones broaden the peaks [21]. The XRD peak shift of the milled samples suggest that the non-uniform microstrain developed at the lattice sites during mechanical process may also contribute such type of peak broadening [7]. In literature the small shift of XRD peak is very often neglected. But a critical observation of this type of shift is very important in correlating the physical properties with mechanical strain induced change in a sample [20].

B. Magnetic properties

The inset of Fig. 2 (left scale) shows the zero field cooled (ZFC) and field cooled (FC) magnetization data for CoRh_2O_4 bulk sample, measured at 100 Oe dc magnetic field. The bulk sample shows antiferromagnetic ordering at $T_N \approx 27.5\text{K} \pm 0.5\text{K}$ and magnetic irreversibility between ZFC and FC magnetization below T_N . The ZFC magnetization data at $T > 50\text{K}$ are well fitted with Curie-Weiss law (Fig.2 inset, right scale)

$$\chi = \frac{C}{T - \theta_A} \quad (1)$$

The Curie constant ($C = N\mu_{eff}^2/3k$, N is the number of CoRh_2O_4 formula unit per gram of the sample) gives the effective magnetic moment ($\mu_{eff} = 4.60 \pm 0.10 \mu_B$) per formula unit for the bulk sample. The asymptotic Curie temperature (θ_A) is $\approx -(45 \pm 2)\text{K}$. These values are consistent with the reported values ($\mu_{eff} = 4.55 \mu_B$) and -30K for bulk CoRh_2O_4 spinel [14]. The negative value of θ_A indicate that on lowering the temperature the antiferromagnetic ordering is saturated at $T_N \approx 27.5\text{K}$ and the system shows strong antiferromagnetic ordering below 27.5K . This indicate the magnetic phase of our bulk CoRh_2O_4 sample is consistent with the reported one. Interestingly, all the milled samples (with smallest particle size $\sim 16\text{ nm}$) are showing (Fig.2, log-log scale) antiferromagnetic ordering at $T_N \approx$

(27.5 ± 0.5)K with magnetic irreversibility between ZFC and FC magnetization when temperature decreases below T_N . The larger value of FC magnetization than ZFC magnetization below T_N suggests the field induced metastable magnetic state during field cooling process of the samples [23]. It is also found that the ZFC magnetization data at $T > 50$ K fit with Curie-Weiss law (Fig.2 inset, right scale), as an example shown for mh60 sample, for all the milled samples. The effective magnetic moment (μ_{eff}) and θ_A values are shown in Table 1. We see that the effective magnetic moment value is increasing with decreasing the particle size. Similar kind of magnetic enhancement was observed by F. Liu et al. [24] and was attributed as a function of the reduction of coordination number of the surface spins when the dimensionality of ferromagnetic particles were reduced. The ratio of θ_A and T_N is always greater than 1. According to ref. [25], if this ratio quantify the degree of magnetic frustration in a geometrically frustrated antiferromagnet, then we can say that geometrical frustration and the instability of antiferromagnetic ordering is increasing with decreasing the particle size by mechanical milling of bulk CoRh_2O_4 spinel. The main characteristic feature is that both the ZFC and FC magnetization are increasing at $T \ll T_N$, which is very similar to paramagnetic or superparamagnetic [26] or ferrimagnetic contribution [15] in the samples. Even, the increase in the magnitude of magnetization below T_N can be assigned due to the increasing number of uncompensated/frustrated spins [27] as the particle size decreases. However, the temperature dependence of inverse of zero field cooled susceptibility (H/M_{ZFC}) at $T < T_N$ shows downward curvature in Fig.3. Interestingly, inset of Fig.3 shows that $H/M_{ZFC} \propto T^\alpha$ below 10K and the constant value α increases with decreasing particle size. This indicates that the magnetization below T_N are something different from a typical paramagnet or superparamagnetic behaviour, where inverse of susceptibility should be linear with temperature and α should be 1. M. Sato et al. [15] suggested similar kind of magnetic behaviour below T_N due to the appearance of ferrimagnetic phase when the particle size of the antiferromagnetic spinel Co_3O_4 was reduced to 15 nm.

The most important feature in Fig.4 is that the excess amount of zero field cooled magne-

tization of milled samples ΔM_{mb} ($= M_{zfc}^{milled} - M_{zfc}^{bulk}$) over the bulk sample not only increases at $T < T_N$, but also depend on the particle size. We have found in Fig.4 inset that ΔM_{mb} vs T follows a scaling law at $T \ll T_N$ in the form

$$\Delta M_{mb} = (\Delta M_{mb})_0 T^{-(0.937 \pm 0.002)} \quad (2)$$

where the constant $(\Delta M_{mb})_0$ depends on the particle size and linearly increases as 8.952×10^{-3} , 1.475×10^{-2} , 2.111×10^{-2} , 2.821×10^{-2} and 3.576×10^{-2} (in emu/g unit) for mh12, mh24, mh36, mh48 and mh60 samples, respectively.

The excess in of FC magnetization over the ZFC magnetization (Fig.5a) ,*i.e.*, $\Delta M_{FZ} = M_{FC} - M_{ZFC}$ increases below T_N in a typical manner which has similar character as the uncompensated interfacial antiferromagnetic spins exhibit in $\text{Ni}_{81}\text{Fe}_{19}/\text{CoO}$ bilayers [28]. In case of spinel oxides, the surface cations have various number of next nearest neighbours on both A and sites. When the particle size are reduced to nanometer range, some of the exchange bonds are broken and coordination number to oxygen ions are also decreased. This results a distribution of net exchange fields, which controll the surface magnetism of the particle [6]. This exchange field is proportional to the spin density of the uncompensated antiferromagnetic spins at the surface [28]. The magnitude of ΔM_{FZ} will depend on the number of uncompensated spins and also the exchange interactions between field aligned (uncompensated surface) spins and the antiferromagnetic core spins. This argument invokes the core/shell picture [6] for our samples, where the shell thickness, consisting of uncompensated spins, is increasing with decreasing the particle size by decreasing the core volume.

The zero field cooled magnetization at 100 Oe, 1 kOe and 1 Tesla field for rh48 sample (particle size ~ 19 nm) (Fig.5b) do not show any appreciable change of T_N with fields. This suggests that dominant antiferromagnetic order (LRAO) still exists for the nano particle samples. However, it is the fact that long range antiferromagnetic ordering is proportional to the divergence of magnetization at T_N . Qualitatively, we can say, LRAO is proportional to the difference between peak magnetization (M_{ZFC}^{peak}) at T_N and minimum of magnetization (M_{ZFC}^{min}) below T_N . Following this argument, we see (Fig.5a, inset) the difference

between peak magnetization and minimum magnetization below T_N , i.e., $\Delta M_{pm} = (M_{ZFC}^{peak} - M_{ZFC}^{min})/M_{ZFC}^{peak}$, reduces from 27% (for bulk sample) to 0.5% (for mh60 sample). This confirms that although antiferromagnetic ordering is still observed below T_N , the magnetic disorder is increasing when the particle size decreases by mechanical milling [19].

Fig.6 shows the zero field cooled magnetization as a function of magnetic field at 5K for all the samples. The straight line nature of M vs H plot for $H = -3T$ to $+7T$ range shows a typical antiferromagnetic bulk sample. The antiferromagnetic nature is still very prominent for mh12 sample. But the downward curvature of the M vs H curve (see for mh36 and mh60 samples) in the positive field range suggests that some magnetic contribution is increasing as the particle size decreases. From the Arrot plot (M^2 vs H/M), we have found no spontaneous magnetization for any samples, whereas the linear extrapolation of the data (for $H \geq 4$ Tesla) to the M axis gives some finite values of M_{0T} for all milled samples. The $M(H)$ data, therefore, confirm that there is no ferromagnetic ordering in the system. The magnetic contribution arising in decreasing the particle size can be attributed as disorder and dilution effect in antiferromagnetic spinel [15]. The increase of M_{0T} (Fig.6 inset) with increasing the milling time indicates that although the samples do not show any ferromagnetic spontaneous magnetization but field induced magnetic ordering is possible for antiferromagnetic nano particles [29]. Fig.7 shows the M vs H data at different temperatures for the 48 hours milled sample. The linear extrapolation of M for $H \geq 4T$ to $H = 0T$ axis shows (Fig. 7 inset) that the magnetization (M_{0T}) first decreases with increasing temperature down to $\approx 16K$ and then increases up to $27K$. The temperature dependence of M_{0T} is very similar to the temperature dependence of magnetization at $T < T_N \approx 27.5K$ for the same sample. This type of magnetic behaviour suggests that there is certainly a competition between antiferromagnetic order and magnetic order due to disorder effect in the nano particle samples [18]. Further, it can be suggested that the disorder effect will dominate as the temperature is well below of T_N .

IV. SUMMARY

The bulk CoRh_2O_4 spinel is an antiferromagnet with ordering temperature $T_N \approx 27.5\text{K}$. When the particles size of CoRh_2O_4 are reduced by mechanical milling, the signature of antiferromagnetic order at $\approx 27.5\text{K}$ are still observed upto particle size $\approx 16\text{ nm}$. In case of nano particles, the magnetization below T_N is enhanced with respect to the bulk sample, which is followed by a scaling law. Since the antiferromagnetic ordering temperature at T_N is unchanged, the enhancement in magnetization can not be attributed due to the site exchange [30] between Co^{2+} and Rh^{3+} ions when the particle size decreases by mechanical milling. Under this circumstances, the tetrahedral (A) sites occupy magnetic Co^{2+} ions and octahedral (B) sites occupy non-magnetic Rh^{3+} ions and excludes the possibility of conventional ferrimagnetic contribution in this system. The temperature dependence of the inverse susceptibility below 10K also suggest that the enhancement of magnetization is not due to typical superparamagnetic contribution of the nano particles.

Therefore, we are introducing the core-shell structure of the nano particles [6]. The core consists of antiferromagnetic spins and shell consists of few layers of surface spins. The surface spins are coupled by superexchange interactions (via O^{2-} ions) to the core spins. In case of bulk sample the length scale of antiferromagnetic interactions can span upto many particles. When the particle size is reduced to nanometer scale by mechanical milling, some of the A-O-A superexchange bonds are broken and become frustrated. These frustrated bonds (surface spins) will create exchange anisotropy field at the interfacial surface [6,28]. This type of anisotropy field will give rise a preferential magnetic ordering of the loosely bound shell spins, whereas the tightly bound core spins will remained as antiferromagnetically aligned.

V. CONCLUSIONS

Based on our dc magnetic measurements, it can be concluded that the total magnetization of the nanoparticle $M = M_{core} + M_{shell}$, where M_{core} is magnetic contribution from core spins and M_{shell} is magnetic contribution from shell spins. The competition between magnetic ordering of shell spins and the antiferromagnetic ordering of core spins guide the magnetic behaviour of our samples. The shell thickness is increasing in-expense of core volume when the particle size decreases. This is related to the decrease of coordination number of the surface (shell) spins and increase of magnetized state of the surface spins due to increasing random exchange fields, as the size of the particle decreases. Consequently, the magnetic moment will be enhanced in nano particles. This is called disorder induced magnetic ordering in antiferromagnetic nano particle.

Acknowledgement: One of the authors RNB thanks Council of Scientific and Industrial Research (CSIR, India) for providing fellowship [F.No.9/489(30)/98-EMR-I].

Table 1. Particle size (from TEM photographs), Lattice parameter (\AA) (from XRD data), 311 peak position (from XRD data), effective magnetic moment (μ_{eff}) (from M vs T data), Asymptotic Curie temperature (θ_A) (from M vs T data) as a function of milling hours.

sample	milling time	particle size	a(\AA)	2θ (deg)	μ_{eff} (μ_B unit)	θ_A (K)
bulk	0h	few μm	8.465 ± 0.002	35.47	4.599	-44.23
mh12	12h	70 ± 1 nm	8.485 ± 0.002	35.56	4.603	-42.80
mh24	24h	50 ± 1 nm	8.427 ± 0.002	35.75	4.609	-42.05
mh36	36h	32 ± 1 nm	8.449 ± 0.002	35.71	4.627	-41.84
mh48	48h	19 ± 1 nm	8.468 ± 0.002	35.67	4.653	-43.81
mh60	60h	16 ± 1 nm	8.459 ± 0.002	35.64	4.755	-51.00

REFERENCES

- [1] D. Leslie-Pelecky and R. D. Rieke, Chem. Mater. **8**, 1770(1996)
- [2] J. Tejada, R. F. Ziolo and X. X. Zhang, Chem. Mater. **8**,1784(1996)
- [3] Magnetic properties of fine particles, edited by J. L. Dorman and D. Fiorani (North-Holand, 1991)
- [4] S. Gangopadhyay, G.C. Hadjipanayis, B. Dale, C. M. Sorensen, K. J. Klabunde, V. Papaefthymiou and A. Kostikas, Phys. Rev. B **45**, 9778 (1992)
- [5] R. H. Kodama and A. E. Berkowitz, Phys. Rev. B **59**, 6321 (1999)
- [6] R. H. Kodama, A. E. Berkowitz, E. J. McNiff. Jr and S. Foner, Phys. Rev. Lett. **77**, (1996)p.394
- [7] L. Bianco, A. Hernando, E. Bonetti and E. Navarro, Phys. Rev. B **56**, 8894(1997)
- [8] H. H. Hamdeh, J. C. Ho, S. A. Oliver, R. J. Willey, G. Oliveri and G. Busca, J. Appl. Phys. **81**, 1851(1997)
- [9] X. Batlle and A. Labarta, J. Phys. D: Appl. Phys. **35**, R15 (2002)
- [10] V. sepelak, S. Wißmann and K. d. Becker, J. Magn. Magn. Mater. **203**, 135(1999)
- [11] S. A. Oliver, H. H. Hamdeh and J. C. Ho, Phys. Rev. B **60**, 3400(1999)
- [12] Z. X. Tang, C. M. Sorensen, K. J. Klabunde and G. C. Hadjipanayis, Phys. Rev. Lett. **67**, 3602(1991)
- [13] V. A. M. Brabers, Hand book of Magnetic Materials, edited by K. H. buschow **8**, 189(1995); S. Krupika and P. Novak, Ferromagnetic Materials, edited by E. P. Wolfarth, North-Holand publishing company **3**, 189(1982)
- [14] G. Blasse and D.J. Schipper, Phys. Lett. **5**, 300(1963)
- [15] M. Sato, S. Kohiki, Y. Hayakawa, Y. Sonda, T. Babasaki, H. Deguchi and M. Mitome,

- J. Appl. Phys. **88**, 2771 (2000)
- [16] M.E. Zhitomirosky, A. Honecker and O.A. Petrenko, Phys. Rev. Lett. **85**, 3269 (2000)
- [17] J. Villain, Z. Phys. B **33**, 31 (1978)
- [18] C. L. Henley, Phys. Rev. Lett. **62**, 2056 (1989)
- [19] H. Reichert, V.N. Bugaev, O. Shchyglo, A. Schöps, Y. Sikula and H. Dosch, Phys. Rev. Lett. **87**, 236105 (2001)
- [20] R.N.Bhowmik and R. Ranganathan, J. Mater. Sc. (in press)
- [21] B. D. Cillity, Elements of X-Ray Diffraction (second edition), Addison-Wesley Publishing Company, Inc (1977)
- [22] C.N. Chinmasamy, A.Narayanasamy, N. Ponpandian, K. Chattopadhyay, H. Guerault and J-M Greneches, J. Phys.: Condens. Matter **12**, 7795 (2000)
- [23] J. Mattsson, C. Djurberg and P. Nordblad, Phys. Rev. B **61**, 11274 (2000)
- [24] F. Liu, M.R. Press, S. K. Khanna and P. Jena, Phys. Rev. B **39**, 6914(1989)
- [25] S.E. palmer and J.T. Chalker, Phys. Rev. B **62**, 488 (2000)
- [26] D. Fiorani and S. Viticoli, J. Magn. Magn. Mater. **49**, 83(1985)
- [27] M.S. Seehra and A. Punnoose, Phy. Rev. B **64**, 132410 (2001)
- [28] K. Takano, R.H. Kodama, A.E. Berkowitz, W. Cao and G. Thomas, J. Appl. Phys. **83**, 6888(1998)
- [29] M.E. Zhitomirsky, A. Honecker and O.A. Petrenko, Phys. Rev. Lett. **85**, 3269 (2000)
- [30] V. A. M. Brabers, Phys. Rev. Lett. **68**, 3113(1992)

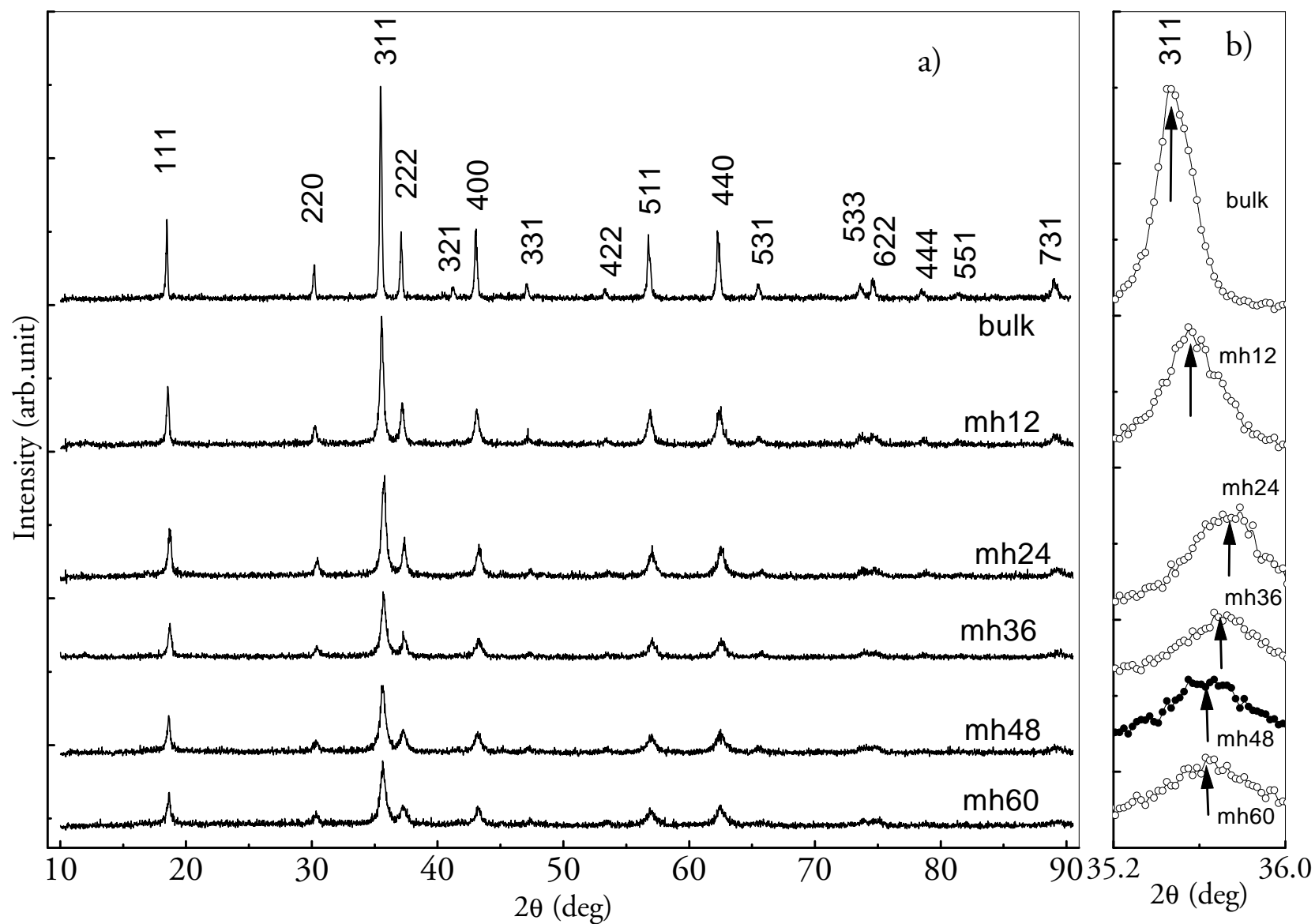


Fig.1 a) shows the XRD spectra of bulk and milled (mh12, mh24, mh36, mh48 and mh60) samples.

b) shows the 311 peak of XRD spectra. The arrow indicates the position of 311 peak.

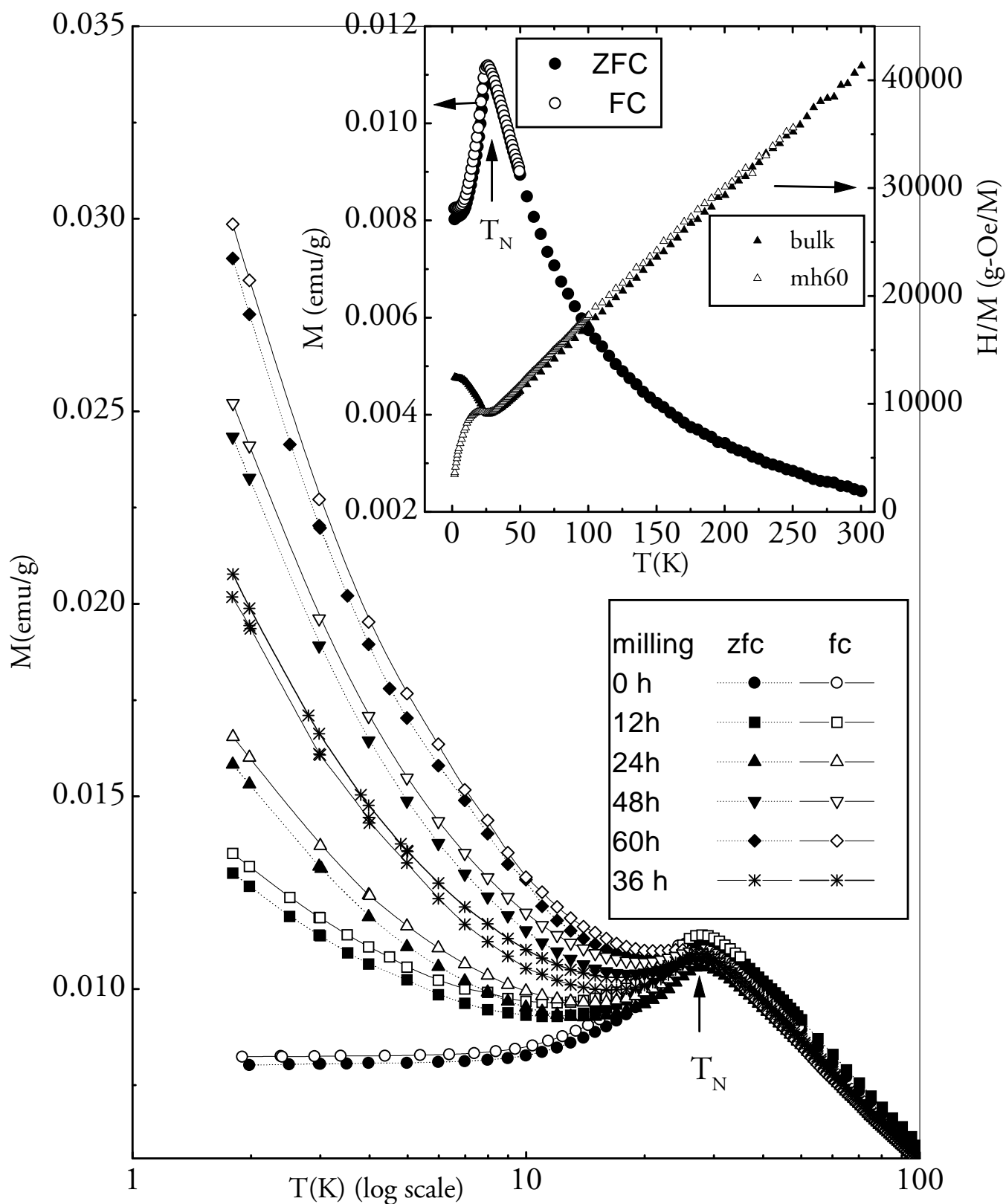


Fig. 2. Inset (left scale) shows the ZFC and FC magnetization at $H = 100$ Oe for bulk sample. Inset (right scale) shows H/M for bulk and mh60 samples for $H = 100$ Oe. The main panel shows the ZFC and FC magnetization for bulk, mh12, mh24, mh36, mh48 and mh60 samples at $H = 100$ Oe. T_N represent the antiferromagnetic ordering temperature. Solid and dotted lines guide to eye

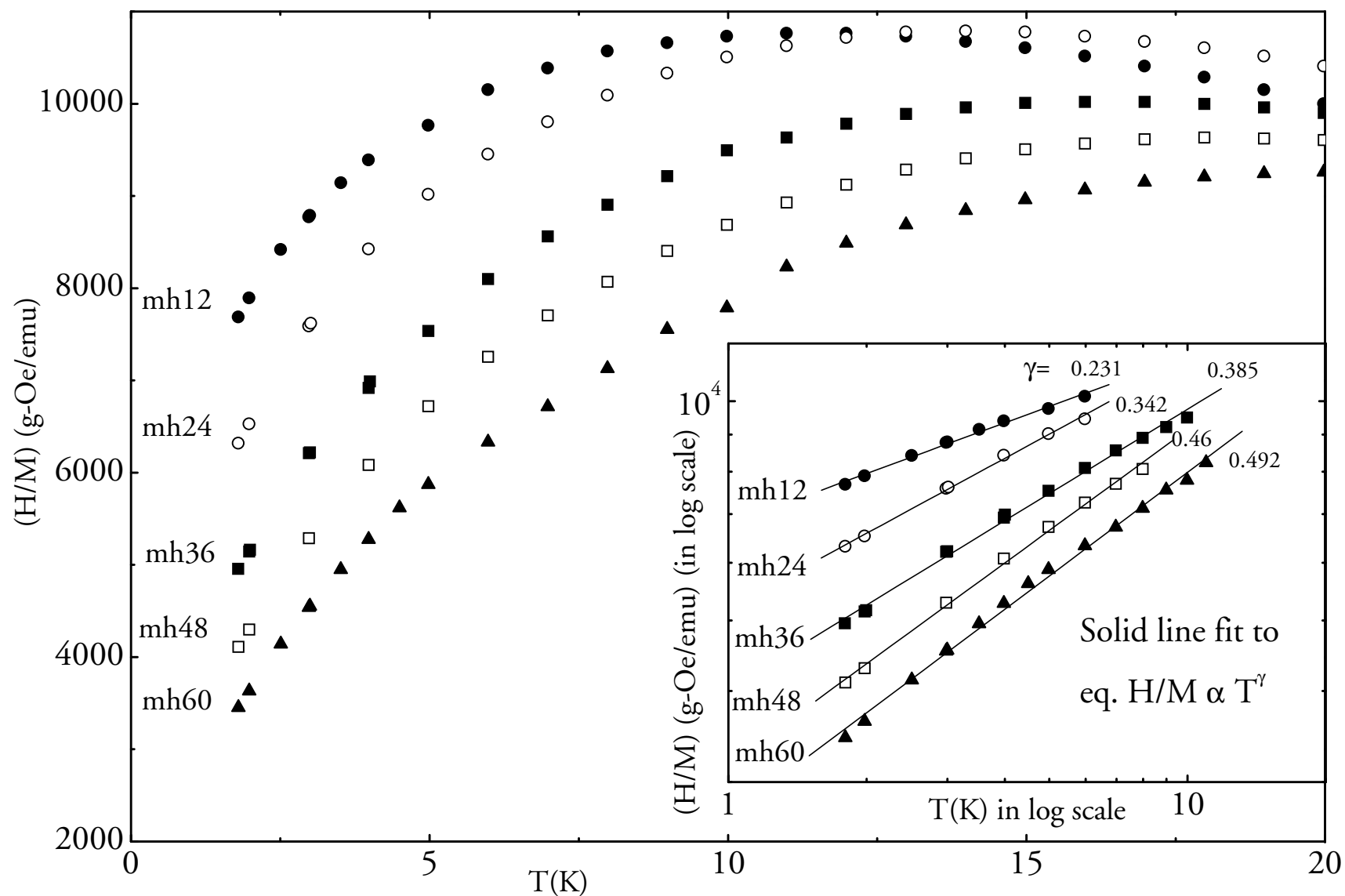


Fig.3 Temperature dependence of inverse zero field cooled susceptibility ($H=100$ Oe/ M_{ZFC}) for milled samples. The inset shows the experimental data (point symbol) and fit data (lines)

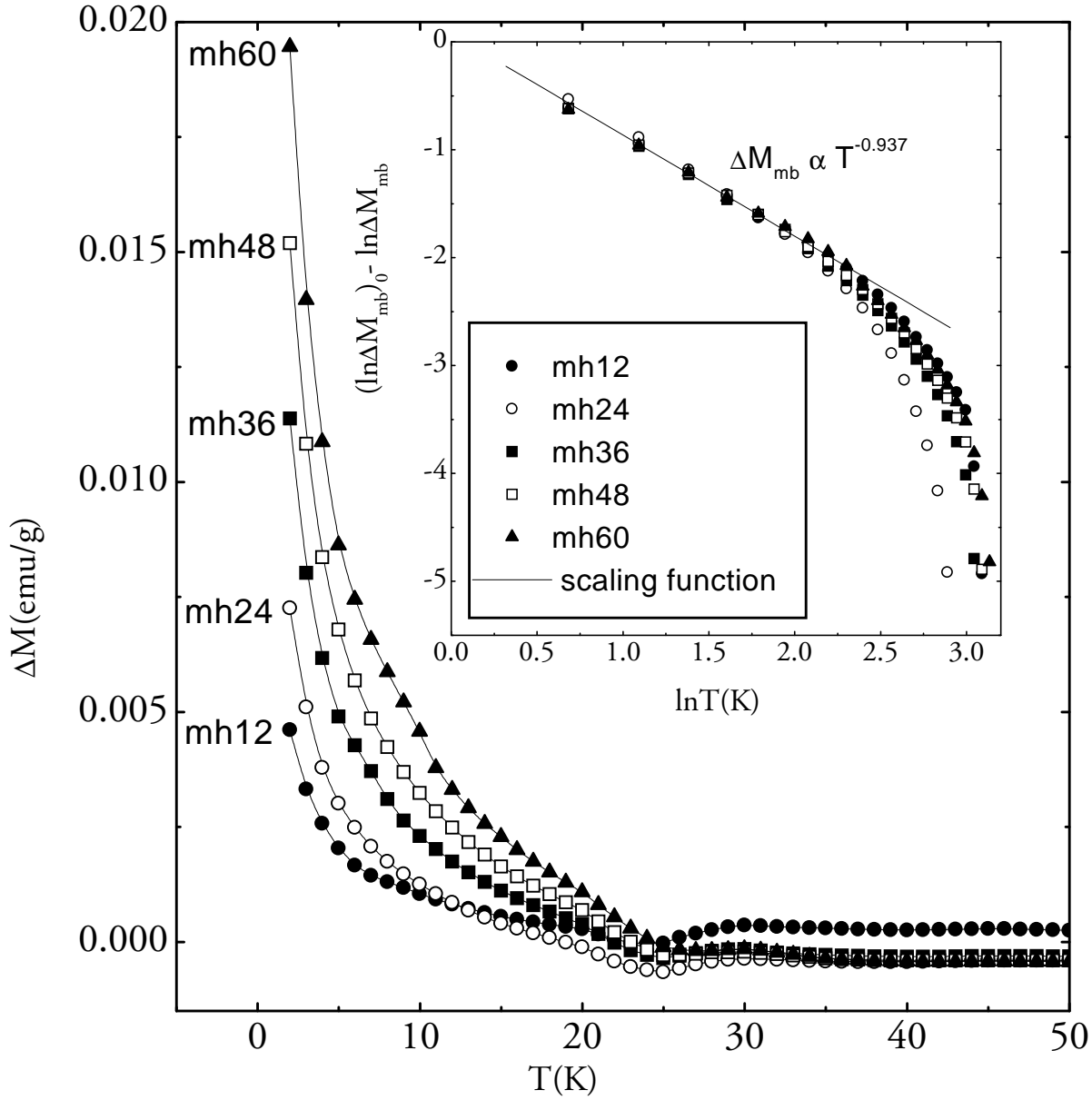


Fig. 4 Temperature dependence of the excess ZFC magnetization of milled samples, measured at $H = 100$ Oe, over bulk sample. The inset shows the expt data (points) and fit data (line) to eq. (2)

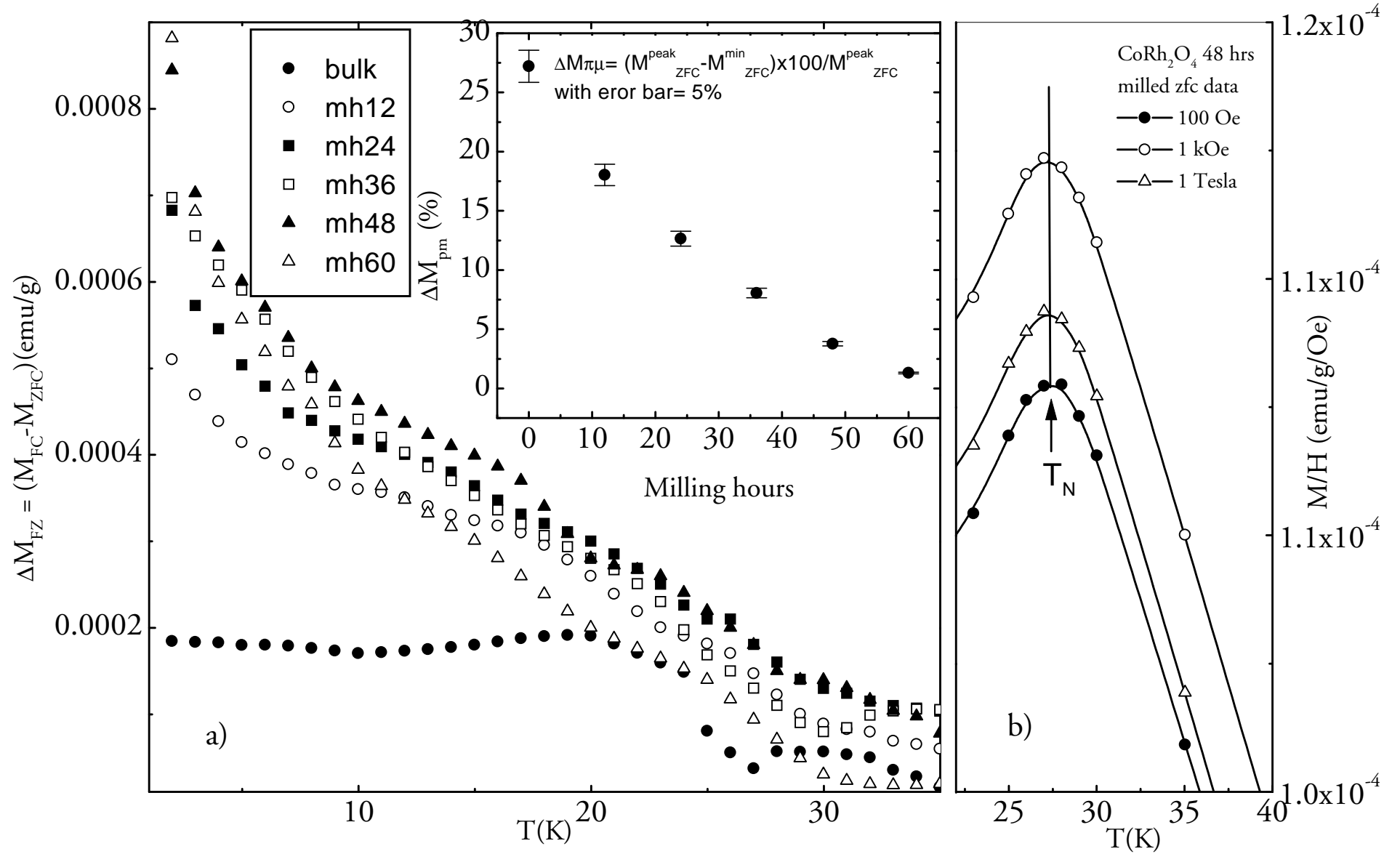


Fig.5 a) The temperature dependence of excess FC magnetization over ZFC magnetization for all bulk and milled samples. The inset shows the % change of ZFC peak magnetization at T_N over the minimum ZFC magnetization at approx. 15K. b) zero field cooled M/H vs T at $H = 100$ Oe, 1 kOe and 1 Tesla for 48 hrs milled (mh48) sample.

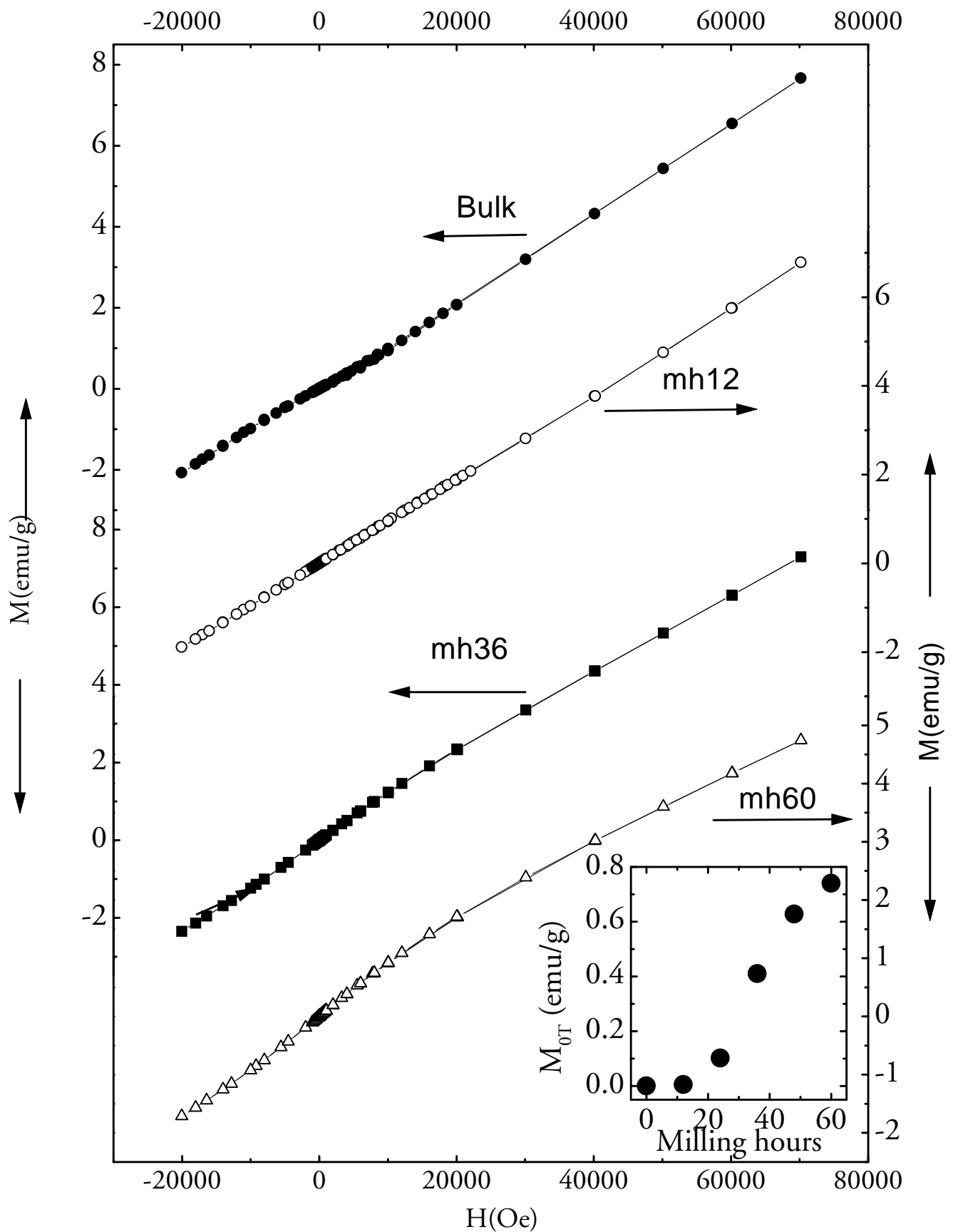


Fig.6 M vs H (in the range: -3 T to 7 T) for bulk, mh12, mh 36 and mh 60 CoRh_2O_4 samples. left and right arrow indicate the M axis for the corresponding sample. The inset shows the linear extrapolation of M at $H > 4\text{ T}$ to $H = 0\text{ T}$ value

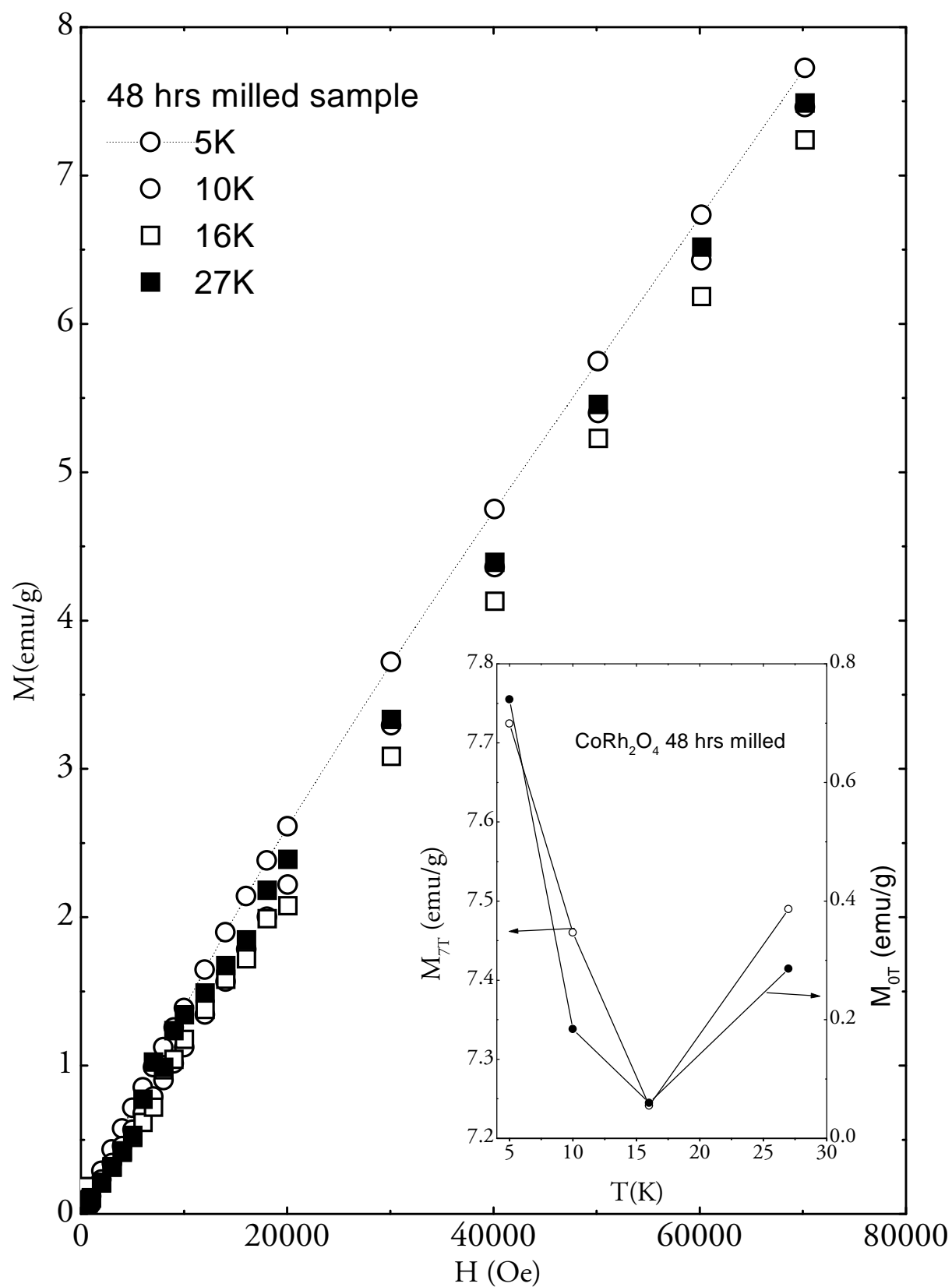


Fig.7 M vs H for 48 hrs milled (mh48) sample. The inset shows the magnetization at 7T and linear extrapolation of M (for $H > 4T$) data to 0T.